

Formation of CF₃O – in the gas phase

Robert A. Morris, Thomas M. Miller, John F. Paulson, A. A. Viggiano, Michael T. Feldmann, Rollin A. King, and Henry F. Schaefer III

Citation: *The Journal of Chemical Physics* **110**, 8436 (1999); doi: 10.1063/1.478753

View online: <http://dx.doi.org/10.1063/1.478753>

View Table of Contents: <http://scitation.aip.org/content/aip/journal/jcp/110/17?ver=pdfcov>

Published by the [AIP Publishing](#)

Articles you may be interested in

Experimental and ab initio studies of the reactive processes in gas phase i-C₃H₇Br and i-C₃H₇OH collisions with potassium ions

J. Chem. Phys. **141**, 164310 (2014); 10.1063/1.4898377

Experimental study of the reactive processes in the gas phase K⁺ + i-C₃H₇Cl collisions: A comparison with Li and Na ions

J. Chem. Phys. **138**, 184310 (2013); 10.1063/1.4804188

Observation of dihalide elimination upon electron attachment to oxalyl chloride and oxalyl bromide, 300 – 550 K

J. Chem. Phys. **124**, 184313 (2006); 10.1063/1.2196409

Trajectory studies of S_N2 nucleophilic substitution. IX. Microscopic reaction pathways and kinetics for Cl⁻ + CH₃Br

J. Chem. Phys. **118**, 2688 (2003); 10.1063/1.1535890

Reaction on the O⁻ + CH₄ potential energy surface: Dependence on translational and internal energy and on isotopic composition, 93–1313 K

J. Chem. Phys. **106**, 8455 (1997); 10.1063/1.473904



Formation of CF_3O^- in the gas phase

Robert A. Morris,^{a)} Thomas M. Miller,^{b)} John F. Paulson, and A. A. Viggiano
*Air Force Research Laboratory, Space Vehicles Directorate (AFRL/VSBP), 29 Randolph Road,
Hanscom Air Force Base, Massachusetts 01731-3010*

Michael T. Feldmann, Rollin A. King, and Henry F. Schaefer III
*Center for Computational Quantum Chemistry, Department of Chemistry, University of Georgia, Athens,
Georgia 30602-2525*

(Received 16 November 1998; accepted 2 February 1999)

We report experimental studies of the formation of CF_3O^- by ion-molecule and electron attachment reactions, and theoretical investigations of the structure and energetics of CF_3O^- and its neutral counterpart CF_3O . The anion CF_3O^- is formed from the rapid attachment of free electrons to its neutral dimer, $(\text{CF}_3\text{O})_2$. Potential sources of CF_3O^- through ion-molecule reactions of CF_3^- and F^- were surveyed. CF_3O^- is formed in the bimolecular ion-molecule reaction of CF_3^- with SO_2 and the third-order association reaction of F^- with CF_2O . In addition, rate constants for the reactions of CF_3^- with a variety of neutral compounds were measured. A number of cases were found in which formation of CF_3O^- was energetically allowed but was not observed. The potential energy surfaces of CF_3O and CF_3O^- have been investigated using a variety of density functional theory (DFT) techniques. The ground-state minimum energy structure of CF_3O was found to be a ${}^2A'$ Jahn–Teller distorted C_s -symmetry structure, while for the anion the ground state is 1A_1 with a C_{3v} -symmetry minimum. A search for other low-energy minima for CF_3O^- was unsuccessful. The DFT methods support a value for the adiabatic electron affinity of CF_3O near 4.1 eV. © 1999 American Institute of Physics. [S0021-9606(99)01117-4]

I. INTRODUCTION

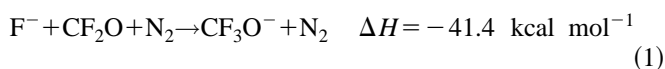
The CF_3O^- anion has been used as a chemical ionization agent for the detection of trace gas phase species in the atmosphere. It reacts with a variety of compounds by fluoride transfer, and Huey *et al.*¹ have reported laboratory kinetics results for such chemical ionization reactions of CF_3O^- with trace gases of interest in atmospheric chemistry. Arijs and Kopp² have used CF_3O^- as a chemical ionization agent in the stratosphere for detection of nitric acid. Thus there is practical interest in determining efficient and convenient means of forming the CF_3O^- anion and for understanding the energetics of CF_3O^- and related species. The neutral CF_3O radical has been suggested to play a role in catalytic ozone destruction cycles in the stratosphere.^{3,4}

There is also fundamental interest in the ability of computational chemistry techniques to faithfully describe the structure and energetics of anions, their neutral counterparts, and the corresponding potential energy surfaces. In particular, the computation of electron affinities and the structural changes involved when an electron is added to a molecule is an important capability in chemical physics. Recently density functional theory has been used to investigate these questions for a growing number of systems and has provided results which are generally in good agreement with experiment.^{5,6}

II. EXPERIMENT

A. Selected ion flow tube

Gas phase kinetics measurements of ion-molecule reactions were made at 300 K under thermal conditions using the selected ion flow tube (SIFT) instrument at the Air Force Research Laboratory (AFRL). The apparatus and technique are standard and have been described previously.⁷ The CF_3^- and F^- reactant ions were formed in a remote electron impact ion source from $\text{C}_3\text{F}_6\text{O}$ (hexafluoropropene oxide) and SF_6 , respectively. The reactant ion of interest was mass selected in a quadrupole mass filter and injected through a Venturi inlet into a fast flow of He buffer gas in a 1-m-long stainless steel flow tube. Nitrogen buffer was used in the experiments on the association reaction of F^- with CF_2O . The ions were transported by the buffer past an inlet through which the reactant neutral was added. The reactant and product ions were sampled through an aperture by a second quadrupole mass spectrometer and detected by pulse counting in a particle multiplier. Reaction rate constants were calculated from the pseudo-first-order attenuation in reactant ion signal as a function of reactant neutral concentration in combination with the measured reaction time. Neutral reactant compounds were obtained commercially and used without further purification. For the reaction of F^- with CF_2O ,



rate constants were measured as a function of pressure (in an N_2 buffer) over the range 0.22–0.60 Torr by throttling a valve in the main flow tube pumping line. All of the reported rate constants are accurate to within $\pm 30\%$.

^{a)} Author to whom correspondence should be addressed; Electronic mail: morris@plh.af.mil

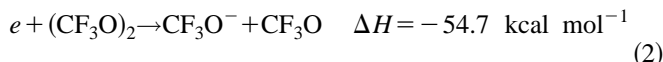
^{b)} Under contract F19628-95-C-0020 to Visidyne, Inc., Burlington, MA.

TABLE I. Second-order rate constants (k_2) for reactions of CF_3^- with selected neutrals measured in ~ 0.4 Torr helium gas. The estimated accuracy is $\pm 30\%$.

Reaction	ΔH (kJ mol $^{-1}$)	k_2 (cm 3 s $^{-1}$)
$\text{CF}_3^- + \text{SO}_2 \rightarrow \text{CF}_3\text{O}^- + \text{SO}$	-112	7.5×10^{-10}
$\text{CF}_3^- + \text{NO}_2 \rightarrow \text{NO}_2^- + \text{CF}_3$	-189	4.2×10^{-10}
$\text{CF}_3^- + \text{CO}_2 \rightarrow \text{CF}_3\text{CO}_2^-$	-168	1×10^{-11}
$\text{CF}_3^- + \text{HCl} \rightarrow \text{Cl}^- + \text{CF}_3\text{H}$	-182	1.1×10^{-9}
$\text{CF}_3^- + \text{HBr} \rightarrow \text{Br}^- + \text{CF}_3\text{H}$	-224	4.3×10^{-10}
$\text{CF}_3^- + \text{CH}_3\text{Cl} \rightarrow \text{Cl}^- + \text{CF}_3\text{CH}_3$	-246	6.5×10^{-11}
$\text{CF}_3^- + \text{CH}_3\text{Br} \rightarrow \text{Br}^- + \text{CF}_3\text{CH}_3$	-276	4.5×10^{-10}
$\text{CF}_3^- + \text{CF}_3\text{Br} \rightarrow \text{Br}^- + \text{C}_2\text{F}_6$	-213	1.6×10^{-11}
$\text{CF}_3^- + \text{SiF}_4 \rightarrow \text{SiF}_5^- + \text{CF}_2$	-57	6.1×10^{-10}
$\text{CF}_3^- + \text{OCS} \rightarrow \text{CF}_3\text{S}^- + \text{CO}$ (15%)	?	5.0×10^{-10}
$\rightarrow \text{CF}_3\text{OCS}^-$ (85%)	?	

B. Flowing afterglow Langmuir probe

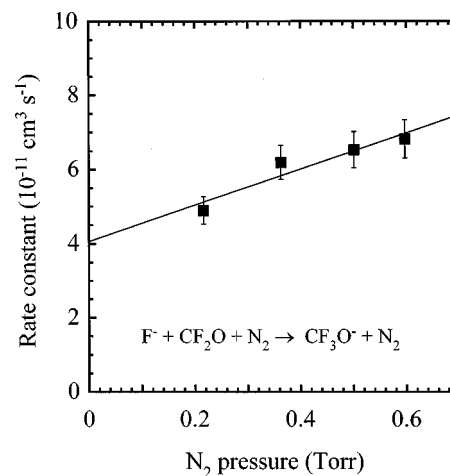
Measurements of rate constants for attachment of free electrons to $(\text{CF}_3\text{O})_2$,



were performed in a variable-temperature flowing afterglow Langmuir probe (FALP) apparatus⁸ at AFRL. The reaction enthalpy was calculated from the dimer bond strength (46.8 kcal mol $^{-1}$)⁹ and the electron affinity of CF_3O (present calculations). The FALP technique¹⁰ has been well described in the literature. The decay in electron density down the axis of a flow tube due to the coupled effects of electron attachment and ambipolar diffusion is measured using the FALP method. This information, together with measurements of the plasma velocity and reactant gas concentration, allows us to deduce the electron attachment rate constant. Mass spectrometric sampling at the downstream end of the flow tube showed that the only product ion was CF_3O^- over the entire temperature range 297–553 K, in 1 Torr helium gas. The $(\text{CF}_3\text{O})_2$ was synthesized and provided by Professor Darryl DesMarteau. Infrared (IR) analysis of the $(\text{CF}_3\text{O})_2$ sample at Clemson University showed that it contained a small amount of COF_2 and possibly CO_2 (neither of which attach electrons in our temperature range). The $(\text{CF}_3\text{O})_2$ sample was degassed at 77 K prior to use. Mixtures of $(\text{CF}_3\text{O})_2$ in He gas were prepared at fractions between 0.6 and 1.0% to facilitate accurate flow measurements of the reactant gas into the FALP apparatus. Daily passivation of the flowmeter and feedline was required, as evidenced by an increase in the apparent attachment rate constant with time, asymptotically

TABLE II. Rate constant upper limits for neutrals unreactive with CF_3^- in ~ 0.4 Torr helium gas.

System	k_2 (cm 3 s $^{-1}$)
$\text{CF}_3^- + \text{O}_2$	$< 6 \times 10^{-13}$
$\text{CF}_3^- + \text{CO}$	$< 1 \times 10^{-12}$
$\text{CF}_3^- + \text{N}_2\text{O}$	$< 8 \times 10^{-13}$
$\text{CF}_3^- + \text{SF}_6$	$< 1 \times 10^{-12}$
$\text{CF}_3^- + \text{CF}_3\text{Cl}$	$< 2 \times 10^{-12}$

FIG. 1. Second-order rate constants for the association reaction of F^- with CF_2O plotted as a function of N_2 buffer gas pressure. The error bars represent estimated relative error limits.

approaching a limiting value. Passivation required nearly an hour of flowing the 1% $(\text{CF}_3\text{O})_2$ mixture, or a few minutes of flowing neat SF_4 gas.

III. EXPERIMENTAL RESULTS

A. Ion-molecule reactions

Reaction rate constants and products of the systems involving CF_3^- which were found to be reactive are given in Table I, and nonreactive cases are listed in Table II along with upper limits to the rate constants. Reported thermochemistry (other than the present computational results) is based on data from NIST.¹¹ In this survey, the only reaction of CF_3^- which was found to produce CF_3O^- was an O atom transfer reaction between CF_3^- and SO_2 , a reaction with a large rate constant. Exothermic formation of CF_3O^- was possible for all the other oxygen-containing reactant neutrals studied (except for CO) but was not observed.

Other reactions of CF_3^- involved charge transfer, atom transfer, displacement, fluoride transfer, and association, as seen in Table I. The fast charge transfer reaction to NO_2 confirms that the adiabatic electron affinity of the CF_3 radical is less than the 2.273 eV value known¹² for NO_2 . The reaction of CF_3^- with CO_2 proceeds entirely by association, despite the fact that formation of CF_3O^- is exothermic by 31.3 kcal mol $^{-1}$. CF_3^- reacts by halide displacement with the acids HCl and HBr and with the methyl halides CH_3Cl and CH_3Br , with faster rates for the bromides. The reaction with CF_3Br is inefficient and proceeds by bromide displacement. CF_3^- effi-

TABLE III. Rate constants (k_a) for electron attachment to $(\text{CF}_3\text{O})_2$ as a function of temperature. The estimated accuracy is $\pm 30\%$.

T (K)	k_a (10^{-8} cm 3 s $^{-1}$)
297	0.92
363	1.2
424	1.3
494	1.5
553	1.8

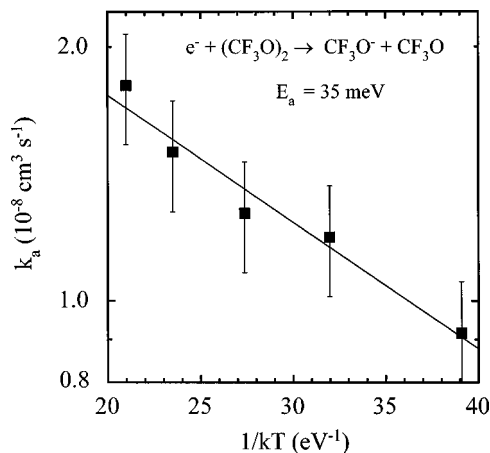


FIG. 2. Arrhenius plot of the rate constants for electron attachment to $(\text{CF}_3\text{O})_2$. The error bars represent estimated relative error limits.

ciently transfers fluoride to SiF_4 . The reaction with OCS is fast and displays both atom transfer and association reaction channels, while the energetically allowed formation of CF_3O^- was not observed.

The association reaction of F^- with CF_2O , forming CF_3O^- [Reaction (1)], was studied as a function of pressure in N_2 buffer from 0.22 to 0.6 Torr at 300 K. The second-order rate constants are plotted as a function of pressure in Fig. 1. The data fall on a straight line within the relative error bars (shown as $\pm 7.5\%$). However, the intercept is distinctly nonzero. This implies that there is either a radiative component to the association reaction or that fall-off behavior is applicable. The limited pressure range is not sufficient to distinguish between these two possibilities. If radiative association is the reason for the nonzero intercept, the radiative component of the second-order rate constant is derived from the intercept and is $4.1 \times 10^{-11} \text{ cm}^3 \text{ s}^{-1}$. In this scenario the slope is the third-order rate constant, equal to $1.5 \times 10^{-27} \text{ cm}^6 \text{ s}^{-1}$.

B. Electron attachment

Results from the electron attachment experiments are given in Table III. Each datum is the average of 2–4 runs at different $(\text{CF}_3\text{O})_2$ concentrations. At room temperature the electron attachment rate constant for Reaction 2 is $9.2 \times 10^{-9} \text{ cm}^3 \text{ s}^{-1}$, which corresponds to one attachment event in roughly every 30 collisions.¹³ An Arrhenius-type plot of the data is shown in Fig. 2. The rate constants can be fit with the expression $k_2 = 3.5 \times 10^{-8} \text{ cm}^3 \text{ s}^{-1} \exp(-0.036 \text{ eV}/kT)$ over this limited temperature range, where k_2 is the attachment rate constant. The 36 meV activation energy in this expression is likely related to energy given up by the incoming electron to induce vibrations in $(\text{CF}_3\text{O})_2$ which enhance bond scission and promote electron attachment. Observation of CF_3O^- as the only ionic product of attachment at thermal energies is consistent with the earlier electron-beam work of MacNeil and Thynne.¹⁴ F^- was also seen at zero electron energy in the earlier work, but was attributed to interaction with a hot filament in the apparatus.

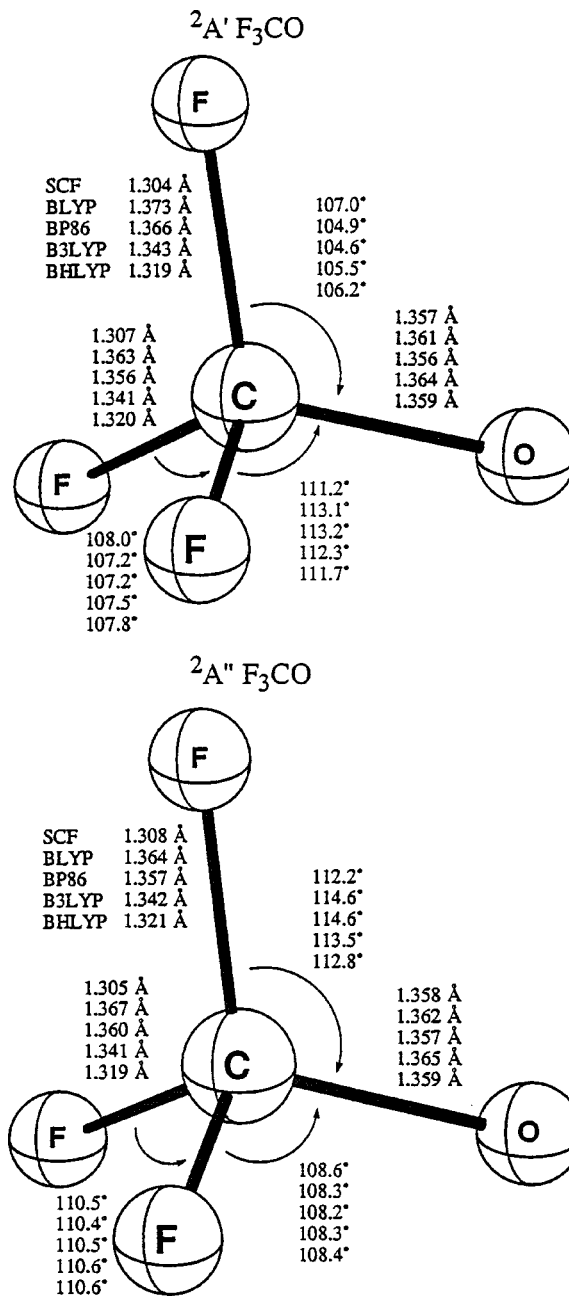


FIG. 3. Optimized geometries for the C_s -symmetry ${}^2A'$ minimum and the ${}^2A''$ transition state of CF_3O .

C. Theoretical methods

The quantum chemical computations have been executed using the PSI 2.0 program package¹⁵ to complete spin-restricted closed-shell Hartree Fock (RHF) and spin-restricted open-shell Hartree Fock (ROHF) computations and the GAUSSIAN 94 program system¹⁶ to complete the density functional theory (DFT) computations. The DFT methods used were the BLYP, B3LYP, BP86, and BHLYP methods. The BLYP method uses Becke's 1988 exchange functional (B)¹⁷ with the Lee, Yang, and Parr correlation functional (LYP).¹⁸ The B3LYP method is a DFT-HF hybrid method that uses Becke's exchange functional (B3)¹⁹ with the LYP correlation functional. The BP86 method uses the B exchange functional with the correlation correction of Perdew

TABLE IV. Relative energies of the ${}^2A'$ and ${}^2A''$ stationary points of CF_3O in cm^{-1} .^a

	BLYP	BP86	B3LYP	BHLYP	SCF
${}^2A'$ CF_3O	0.0 (0.0)	0.0(0.0)	0.0(0.0)	0.0(0.0)	0.0(0.0)
${}^2A''$ CF_3O	50.7(53.1)	57.1(60.8)	40.2(42.8)	26.1(31.4)	10.8(16.1)

^aAll results were obtained with the DZP^{++} basis set. Values are corrected for ZPVE via the harmonic approximation and the omission of the low frequency CF_2 twist-rock mode from the computation of the ZPVE of each structure. Noncorrected values in parentheses.

(P86).²⁰ Finally, the BHLYP method uses Becke's half-and-half exchange functional (BH)²¹ along with the LYP correlation functional.

The basis set used was the standard double- ζ plus polarization (DZP) basis set augmented with diffuse orbitals, called the DZP^{++} basis set. The DZ part of the basis was constructed from the Huzinaga–Dunning^{22,23} set of contracted Gaussian functions. The DZP basis was formed by the addition of a set of d -type polarization functions constructed using the five pure d components $\{\alpha_d(\text{C})=0.75, \alpha_d(\text{F})=1.00, \alpha_d(\text{O})=0.85\}$. The DZP^{++} basis was constructed by the addition of diffuse functions to the DZP basis. Each atom received one additional s type and one additional set of p -type functions $\{\alpha_s(\text{C})=0.04302, \alpha_p(\text{C})=0.03629, \alpha_s(\text{F})=0.10490, \alpha_p(\text{F})=0.08260, \alpha_s(\text{O})=0.08227, \alpha_p(\text{O})=0.06508\}$. The diffuse function orbital exponents were determined in an "even tempered sense" as a mathematical extension of the primitive set, according to the formula of Lee and Schaefer.²⁴ The contraction scheme for each atom is $10s6p1d/5s3p1d$.

D. Computational results

The structures of CF_3O and CF_3O^- have previously been studied computationally with ROHF and RHF wave functions and a 3-21G basis set.²⁵ A more recent study of the CF_3O^- anion reported an optimization within C_{3v} -symmetry constraints at the 6-311++G**RHF level.²⁶ This work, while adding the effects of electron correlation to these previous computations, includes an investigation of a larger portion of the potential energy hypersurface, in search of heretofore undiscovered low-energy minima.

Francisco and Williams²⁵ observed that the 2E state of C_{3v} -symmetry CF_3O is Jahn–Teller distorted, causing CF_3O to have two low-lying C_s -symmetry stationary points corresponding to ${}^2A'$ and ${}^2A''$ electronic states. The computed C_s -symmetry optimized geometries for the ${}^2A'$ and the ${}^2A''$ stationary points are given in Fig. 3. For the ${}^2A'$ stationary point, the pure DFT methods, BLYP and BP86, give an in-plane C–F bond which is larger than the out-of-plane C–F bonds by 0.01 Å, while the BHLYP and self consistent field (SCF) predict the out-of-plane C–F bonds are slightly longer. The reverse situation occurs for the ${}^2A''$ state where only the pure DFT methods predict that the out-of-plane C–F bonds are longer. The Jahn–Teller distortion is clearly very sensitive to differences in the exchange and correlation treatments. The relative energies of the optimized ${}^2A'$ and ${}^2A''$ stationary points are provided in Table IV. For all methods

attempted, the ${}^2A'$ structure is lower in energy, though the DFT methods give an energy difference of only 26–57 cm^{-1} .

The DFT harmonic vibrational frequencies for the ${}^2A'$ and ${}^2A''$ stationary points are included in Table V. The DFT

TABLE V. Harmonic vibrational frequencies in cm^{-1} computed with the DZP^{++} basis set.^a

	SCF	BLYP	BP86	B3LYP	BHLYP	Experimental
$\text{CF}_3\text{O } {}^2A'$						
$a'(a_1)$	1455	1157	1192	1252	1356 (353)	
C–O stretch						
$a''(e)$	1421	1081	1115	1200	1316 (433)	1221.6 ^b
C–F stretch						
$a'(e)$	1415	1010	1042	1164	1303 (371)	
C–F stretch						
$a'(a_1)$	991	835	852	886	944 (3)	907 ^c
C–F stretch						
$a'(a_1)$	687	573	582	608	646 (14)	
C–F ₃ bend						
$a''(e)$	658	551	560	585	621 (3)	
CF_2 twist						
$a'(e)$	648	532	538	566	605 (12)	
CF_2 scissor						
$a'(e)$	465	366	367	396	429 (1)	483 ^c
CF_2 wag						
$a''(e)$	233	234	245	252	253 (2)	
CF_2 rock						
$\text{CF}_3\text{O } {}^2A''$						
$a'(a_1)$	1454	1154	1168	1247	1352 (327)	
C–O stretch						
$a'(e)$	1423	1062	1093	1189	1309 (410)	
C–F stretch						
$a''(e)$	1413	1027	1061	1176	1310 (404)	
C–F stretch						
$a'(a_1)$	991	835	852	887	943 (3)	
C–F stretch						
$a'(a_1)$	687	574	582	608	646 (13)	
C–F ₃ bend						
$a'(e)$	672	563	571	597	634 (5)	
CF_2 scissor						
$a''(e)$	632	519	525	553	590 (8)	
CF_2 twist						
$a'(e)$	457	368	371	395	424 (<1)	
CF_2 wag						
$a''(e)$	262i	262i	273i	283i	284i	
CF_2 rock						
$\text{CF}_2\text{OF } {}^2A'$						
a'	1767	1793	1888	2061	648)	
C–O stretch						
a'	1219	1256	1291	1363	471)	
C–F stretch						
a'	930	950	984	1041	63)	
C–F stretch						
a'' F ₂ C–O	714	723	760	812	49)	
out-of-plane						
a'	592	598	622	647	14)	
CF_2 rock						
a'	548	554	576	605	7)	
CF_2 scissor						
a'	250	259	206	101	2)	
O–F stretch						
a'	123	128	104	33	<1)	
C–O–F bend						
a'' F–C–O–F	57	58	50	27	<1)	
torsion						

TABLE V. (Continued.)

$\text{CF}_3\text{O}^- A_1$						Matrix ^d	Crystal ^e
a_1	1685	1614	1629	1648	1680 (881)	1514	1560
C–O stretch							
e	1079	805	832	883	983 (508)	919, 1039	960
C–F stretch							
a_1	923	721	743	784	859 (107)	808	813
C–F stretch							
a_1	670	524	538	570	621 (<1)		595
C–F ₃ bend							
e bend	655	484	505	541	603 (15)	555	576
e bend	465	369	377	398	431 (<1)		422

^aExperimental frequencies are fundamentals. Intensities in km mol^{-1} are reported in parentheses for BHLYP. Irreducible representations in parentheses are those of the vibrational modes in the C_{3v} -symmetry point group.

^bReferences 30 and 31.

^cReference 29.

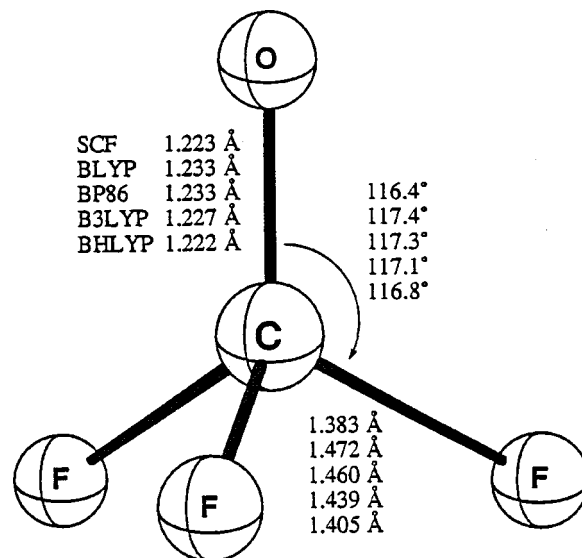
^dReference 35.

^eReference 34.

methods consistently show the ${}^2A'$ stationary point is a minimum energy structure, and the ${}^2A''$ stationary point, possessing one imaginary vibrational frequency, is a transition state. A detailed description of the analogous situation for CH_3O has been given by Colwell, Amos, and Handy.²⁷ There are actually three equivalent ${}^2A'$ minima and three equivalent ${}^2A''$ transition states for CF_3O , each set arising from a distinct plane of symmetry in the C_{3v} point group. Each of the ${}^2A''$ stationary points is a transition state for the interconversion of equivalent ${}^2A'$ minima.

A laser induced fluorescence study of CF_3O in a supersonic jet has produced a high resolution spectrum of the origin band of the $\tilde{A} \leftarrow \tilde{X}$ transition.²⁸ The rotational band progressions were concluded to indicate a C_{3v} -symmetry 2E ground state structure. Another laser induced fluorescence experiment²⁹ has assigned a value of 907 cm^{-1} to the C–F symmetric stretching mode and 483 cm^{-1} to a F–C–O bending mode. The former is in good agreement with the B3LYP value of 886 cm^{-1} while the latter is significantly larger than the usually reliable B3LYP frequency of 396 cm^{-1} . Also, matrix infrared spectroscopy experiments^{30,31} have provided an experimental antisymmetric C–F stretching frequency of 1221.6 cm^{-1} which is consistent with the B3LYP prediction of 1200 cm^{-1} . Although the computed vibrational frequencies are harmonic, experience has shown that DFT (and especially B3LYP) harmonic frequencies tend to be close in value to experimental fundamentals.^{32,33}

Other portions of the CF_3O potential energy surface were investigated using the $\text{DZP}^{++}\text{B3LYP}$ level of theory. A C_{2v} -symmetry optimization of $\text{CF}_2\text{O}+\text{F}$, with F on the O end of CF_2O , obtained a stationary point with one b_1 -type ($16i \text{ cm}^{-1}$) and one b_2 -type ($46i \text{ cm}^{-1}$) imaginary vibrational frequency. Displacing and optimizing in the plane of symmetry containing only one fluorine atom resulted in a transition state with one a'' -type ($50i \text{ cm}^{-1}$) imaginary frequency and an energy that was $1.5 \text{ kcal mol}^{-1}$ below the $\text{F}+\text{CF}_2\text{O}$ fragments. This transition state had an O–F bond distance of 2.303 \AA and a C–O–F bond angle of 90.5° . Displacing into C_1 symmetry and optimizing leads to a planar

FIG. 4. Optimized geometry for the C_{3v} -symmetry structure of CF_3O^- .

minimum, with a O–F bond distance of 2.156 \AA and a C–O–F bond angle of 108.5° . This loosely bound structure, relative to the $\text{F}+\text{CF}_2\text{O}$ fragments, has energy -8.89 (BLYP), -8.51 (BP86), -3.78 (B3LYP), and -1.19 kcal mol^{-1} (BHLYP). The structure is unbound at the ROHF level. The computed vibrational frequencies for this weakly bound structure are given in Table V.

CF_3O^- has been experimentally produced in several ways. Electron attachment to $(\text{CF}_3\text{O})_2$ probably produces the C_{3v} -symmetry structure, which is expected to be the most stable isomer of its composition. However, the rapid addition of F^- to CF_2O leaves the type of addition more in doubt. Is the C_{3v} structure of CF_3O^- formed directly or is a relatively weak electrostatically bound $\text{F}^-+\text{CF}_2\text{O}$ structure formed with a barrier to the C_{3v} structure? A third possibility is a stable F_2COF^- structure.

The computed C_{3v} -symmetry optimized geometries of CF_3O^- are given in Fig. 4. Wiberg²⁶ optimized the C_{3v} -symmetry CF_3O^- structure at the $6-311++\text{G}^{**}\text{RHF}$ level and obtained a geometry similar to the RHF results reported here, except for the C–O bond length for which he obtained a shorter length of 1.214 \AA . The harmonic vibrational frequencies of CF_3O^- are provided in Table V.

TABLE VI. Adiabatic and vertical electron affinities computed with the DZP^{++} basis set in eV.^a

	BLYP	BP86	B3LYP	BHLYP	SCF	Expt.
$\text{EA}_{\text{ad}}({}^2A' \text{CF}_3\text{O})$	4.60 (4.59)	4.69 (4.68)	4.60 (4.58)	4.13 (4.11)	2.75 (2.73)	4.26 ± 0.22^b 3.70 ± 0.5^c 3.25 ± 0.14^d
$\text{EA}_{\text{vert}}({}^2A' \text{CF}_3\text{O})$	(3.66)	(3.77)	(3.61)	(3.15)	(1.81)	

^aCorrected for zero-point vibrational energy. Non-corrected values in parentheses.

^bReference 38.

^cReference 39.

^dReference 40.

TABLE VII. Bond dissociation energies of CF_3O and CF_3O^- in kcal mol^{-1} .^a

	BLYP	BP86	B3LYP	BHLYP	SCF	G2 (0 K) ^b	G2 Free Energy (298 K) ^b	Expt.
² A' $\text{CF}_3\text{O} \rightarrow \text{CF}_2\text{O} + \text{F}$	25.1 (26.0)	27.8 (28.8)	25.0 (26.1)	25.0 (26.4)	16.3 (17.8)	24.1	16.6	22.9 ± 2.6 ^c
¹ A ₁ $\text{CF}_3\text{O}^- \rightarrow \text{CF}_2\text{O} + \text{F}^-$	46.4 (47.0)	49.3 (50.0)	49.2 (50.0)	52.5 (53.5)	48.5 (49.5)	49.3	41.1	42.6 ± 2.0 ^d

^aResults were obtained with the DZP^{++} basis set and are corrected for ZPVE via the harmonic approximation. Values in parentheses are the uncorrected values.

^bReference 43.

^c $D_{298\text{ K}}$, Ref. 41.

^dReference 38.

Experimental fundamental frequencies are available from crystal³⁴ and from matrix³⁵ investigations. Ion pairing in the latter experiment caused a distortion of CF_3O^- away from the C_{3v} structure, but the correspondence between the observed frequencies and the computed C_{3v} frequencies is still clear. The BHLYP and B3LYP methods give the best agreement with these experimental frequencies.

An investigation of other possible structures was carried out using the $\text{DZP}^{++}\text{B3LYP}$ level of theory. In C_{2v} symmetry, optimization with the F^- on the F_2 side of CF_2O led to a transition state with one imaginary b_1 frequency ($59i\text{ cm}^{-1}$), while optimization with F^- on the O side of CF_2O led to dissociation. Displacements out of the molecular plane into C_s symmetry, followed by optimization, led to the C_{3v} -symmetry structure. No barrier to addition in this plane was found, and no change of orbital occupation for $\text{F}^- + \text{CF}_2\text{O} \rightarrow \text{CF}_3\text{O}^-$ in this plane is required. Optimizations with all atoms in a plane, however, led only to dissociation or to very high-lying transition states, displacing from which into C_1 symmetry led to the C_{3v} -symmetry minimum.

The computed electron affinities of CF_3O are given in Table VI. The DFT adiabatic electron affinities for CF_3O range from 4.13 to 4.69 eV. Past experience^{32,36,37} suggests that the lower end of this range is probably the most accurate. The BHLYP value of 4.13 eV is, in fact, within the error bars of the experimental electron affinities of Larson and McMahan³⁸ as well as Spyrou and co-workers.³⁹ The much lower value of 3.25 eV from Taft *et al.*⁴⁰ is clearly too low. The vertical electron affinities are about 1 eV lower than the adiabatic electron affinities, the adiabatic correction involving an increase in all of the C–F bonds in CF_3O by 0.08–0.10 Å and a contraction of the C–O bond distance by 0.12–0.14 Å.

Bond dissociation energies for CF_3O and CF_3O^- are given in Table VII. Schneider and Wallington⁴¹ recommended a fluorine dissociation energy from CF_3O of $22.9 \pm 2.6\text{ kcal mol}^{-1}$ based on experimental and theoretical data. The DFT computed values agree with the high end of this estimate and range from 25.0 to $27.8\text{ kcal mol}^{-1}$. The DFT fluoride dissociation energies from CF_3O^- are more scattered with a range of 46.4–52.5 kcal mol^{-1} and lie above the experimental value of $42.6 \pm 2.0\text{ kcal mol}^{-1}$.³⁸

IV. CONCLUSIONS

Several methods for generating CF_3O^- were examined. A number of reactions of CF_3^- with oxygenated neutrals were surveyed, but only the reaction of CF_3^- with SO_2 formed CF_3O^- despite the availability of exothermic pathways for most of the other reactant neutrals studied. The association reaction of F^- with CF_2O either has an radiative channel or is in the fall-off region in 0.22–0.6 Torr N_2 gas. The attachment of thermal electrons to $(\text{CF}_3\text{O})_2$ formed CF_3O^- exclusively over the temperature range from 297 to 553 K, and the activation energy derived from this temperature dependence most likely reflects an energy barrier to this process. Thus, several methods of generating CF_3O^- were found.

In order to examine whether the three sources of CF_3O^- produced different isomers, DFT calculations for both CF_3O and CF_3O^- were performed. The DFT geometries and frequencies predict a Jahn–Teller distorted CF_3O , giving rise to C_s -symmetry ²A' minima and ²A'' transition states, a pair corresponding to each plane of symmetry in the C_{3v} point group. For the CF_3O^- anion the ground state is ¹A₁ with a C_{3v} -symmetry minimum. The examination of possible structural isomers of CF_3O^- located several stationary points, but none were shown to be minima by evaluation of their harmonic vibrational frequencies. No transition states were found, or barrier predicted, for addition of F^- in the symmetry plane perpendicular to the molecular plane in C_{2v} -symmetry CF_2O . Therefore, the observation of rapid F^- addition to CF_2O appears to be directly to the C_{3v} -symmetry structure of CF_3O^- .

Thus, CF_3O^- may be synthesized by any of the routes studied here for use as a chemical ionization agent in trace neutral detection. The choice is driven by source gases: SO_2 is readily available and easily handled, but the CF_3^- primary ion is not so convenient to produce without creating possibly troublesome species in a chemical ionization environment. Electron attachment to $(\text{CF}_3\text{O})_2$ is a clean process, forming only CF_3O^- , but the starting compound is not commercially available. CF_2O gas is not so pleasant to use, but is commercially available,⁴² and as we have shown, the adduct with F^- is efficiently formed.

ACKNOWLEDGMENTS

Helpful discussions with Dr. Yukio Yamaguchi, Dr. Wesley Allen, Dr. Amy Stevens Miller, and Dr. John Seeley are gratefully acknowledged. We thank Darryl DesMarteau for supplying the $(\text{CF}_3\text{O})_2$. This research was supported by the United States Air Force Office of Scientific Research under Grant AFOSR 95-1-0057 and Task 2303EP4.

- ¹L. G. Huey, P. W. Villalta, E. J. Dunlea, D. R. Hanson, and C. J. Howard, *J. Phys. Chem.* **100**, 190 (1996).
- ²E. Arijis and E. Kopp (private communication).
- ³M. K. W. Ko, N.-D. Sze, J. M. Rodríguez, D. K. Weistenstein, C. W. Heisey, R. P. Wayne, P. Biggs, C. E. Canosa-mas, H. W. Sidebottom, and J. Treacy, *Geophys. Res. Lett.* **21**, 101 (1994).
- ⁴J. A. Montgomery, H. H. Michels, and J. S. Francisco, *Chem. Phys. Lett.* **220**, 391 (1994).
- ⁵G. S. Tschumper and H. F. Schaeffer, *J. Chem. Phys.* **107**, 2529 (1997).
- ⁶J. C. Rienstra-Kiracofe, D. E. Graham, and H. F. Schaeffer, *Mol. Phys.* **94**, 767 (1998).
- ⁷A. A. Viggiano, R. A. Morris, F. Dale, J. F. Paulson, K. Giles, D. Smith, and T. Su, *J. Chem. Phys.* **93**, 1149 (1990).
- ⁸T. M. Miller, A. E. S. Miller, J. F. Paulson, and X. Liu, *J. Chem. Phys.* **100**, 8841 (1994).
- ⁹J. B. Levy and R. C. Kennedy, *J. Am. Chem. Soc.* **94**, 3302 (1972).
- ¹⁰D. Smith and P. Spanel, *Adv. At., Mol., Opt. Phys.* **32**, 307 (1995).
- ¹¹NIST Standard Reference Database No. 69, Vol., edited by W. G. Mallard and P. J. Linstrom (<http://webbook.nist.gov>) Gaithersburg, 1998 (unpublished).
- ¹²K. M. Ervin, J. Ho, and W. C. Lineberger, *J. Phys. Chem.* **92**, 5405 (1988).
- ¹³C. E. Klots, *Chem. Phys. Lett.* **38**, 61 (1976). A polarizability of 5 Å was assumed for $(\text{CF}_3\text{O})_2$ to estimate the collision cross section.
- ¹⁴K. A. G. MacNeil and J. C. J. Thynne, *Int. J. Mass Spectrom. Ion Phys.* **9**, 135 (1972).
- ¹⁵PSI 2.0.; C. L. Janssen, E. T. Seidl, G. E. Scuseria, T. P. Hamilton, Y. Yamaguchi, R. B. Remington, Y. Xie, G. Vacek, C. D. Sherill, T. D. Crawford, J. T. Fermann, W. D. Allen, B. R. Brooks, G. B. Fitzgerald, D. J. Fox, J. F. Gaw, N. C. Handy, W. D. Laidig, T. J. Lee, R. M. Pitzer, J. E. Rice, P. Saxe, A. C. Scheiner, and H. F. Schaefer. This program is generally available for a handling fee of \$100. (PSITECH, Inc., Watkinsville, GA 30677, 1995).
- ¹⁶GAUSSIAN 94. M. J. Frisch, G. W. Trucks, H. B. Schlegel, P. M. W. Gill, B. G. Johnson, M. A. Robb, J. R. Cheeseman, T. A. Keith, G. A. Petersson, J. A. Montgomery, K. Raghavachari, M. A. Al-Laham, V. G. Zakrzewski, J. V. Ortiz, J. B. Foresman, J. Cioslowski, B. B. Stefanov, A. Nanayakkara, M. Challacombe, C. Y. Peng, P. Y. Ayala, W. Chen, M. W. Wong, J. L. Andres, E. S. Replogle, R. Gomperts, R. L. Martin, D. J. Fox, J. S. Binkley, D. J. DeFrees, J. Baker, J. P. Stewart, M. Head-Gordon, C. Gonzalez, and J. A. Pople (Gaussian, Inc., Pittsburgh, PA, 1995).
- ¹⁷A. D. Becke, *Phys. Rev. A* **38**, 3098 (1988).
- ¹⁸C. Lee, W. Yang, and R. G. Parr, *Phys. Rev. B* **37**, 785 (1988).
- ¹⁹A. D. Becke, *J. Chem. Phys.* **98**, 1372 (1993).
- ²⁰J. P. Perdew, *Phys. Rev. B* **33**, 8822 (1986).
- ²¹A. D. Becke, *J. Chem. Phys.* **98**, 5648 (1993).
- ²²S. Huzinaga, *J. Chem. Phys.* **42**, 1293 (1965).
- ²³T. H. Dunning, *J. Chem. Phys.* **53**, 2823 (1970).
- ²⁴T. J. Lee and H. F. Schaefer, *J. Chem. Phys.* **83**, 1784 (1985).
- ²⁵J. S. Francisco and I. H. Williams, *Chem. Phys. Lett.* **110**, 240 (1984).
- ²⁶K. B. Wiberg, *J. Am. Chem. Soc.* **112**, 3379 (1990).
- ²⁷S. M. Colwell, R. D. Amos, and N. C. Handy, *Chem. Phys. Lett.* **109**, 525 (1984).
- ²⁸X.-Q. Tan, M.-C. Yang, C. C. Carter, J. M. Williamson, T. A. Miller, T. E. Mlsna, J. D. O. Anderson, and D. D. DesMarteau, *J. Phys. Chem.* **98**, 2732 (1994).
- ²⁹Z. Li and J. S. Francisco, *Chem. Phys. Lett.* **186**, 336 (1991).
- ³⁰K. C. Clemitshaw and J. R. Sodeau, *J. Phys. Chem.* **93**, 3552 (1989).
- ³¹L. Andrews, M. Hawkins, and R. Withnall, *Inorg. Chem.* **24**, 4234 (1985).
- ³²R. A. King, V. S. Mastryukov, and H. F. Schaefer, *J. Chem. Phys.* **105**, 6880 (1996).
- ³³A. P. Scott and L. Radom, *J. Phys. Chem.* **100**, 16502 (1996).
- ³⁴K. O. Christie, E. C. Curtix, and C. J. Schack, *Spectrochim. Acta A* **31**, 1035 (1975).
- ³⁵B. S. Ault, *J. Phys. Chem.* **84**, 3448 (1980).
- ³⁶R. A. King, J. M. Galbraith, and H. F. Schaefer, *J. Phys. Chem.* **100**, 6061 (1996).
- ³⁷T. J. V. Huis, J. M. Galbraith, and H. F. Schaefer, *Mol. Phys.* **89**, 607 (1996).
- ³⁸J. W. Larson and T. B. McMahon, *J. Am. Chem. Soc.* **105**, 2944 (1983).
- ³⁹S. M. Spyrou, S. R. Hunter, and L. G. Christophorou, *J. Chem. Phys.* **81**, 4481 (1984).
- ⁴⁰R. W. Taft, I. J. Koppel, R. D. Topsom, and F. Anvia, *J. Am. Chem. Soc.* **112**, 2047 (1990).
- ⁴¹W. F. Schneider and T. J. Wallington, *J. Phys. Chem.* **98**, 7448 (1994).
- ⁴²Oakwood Products, Inc., West Columbia, SC; Lancaster Synthesis, Inc., Windham, NH.
- ⁴³L. A. Curtiss, K. Raghavachari, G. W. Trucks, and J. A. Pople, *J. Chem. Phys.* **94**, 7221 (1991).